

Digital MicroPropulsion*

David H. Lewis, Jr. ^a, Siegfried W. Janson ^b, Ronald B. Cohen ^b,
Erik K. Antonsson ^{c,†}

^a TRW, Space & Technology Group, Space & Technology Division,
One Space Park, Redondo Beach, CA 90278, U.S.A.

^b The Aerospace Corporation, Mechanics & Propulsion Department,
Mechanics & Materials Technology Center,
P.O. Box 92957, Los Angeles CA 90009-2957, U.S.A.

^c California Institute of Technology, Engineering Design Research Laboratory,
1200 East California Blvd., Pasadena, California 91125, U.S.A.
<http://www.design.caltech.edu/micropropulsion/>

The Office of the Assistant to the Secretary of Defense of the United States of America has cleared this document for open publication. All copies should carry the legend: "Distribution Statement 'A', Approved for Public Release – Distribution Unlimited."

Abstract

Arrays of "Digital Propulsion" micro-thrusters have been fabricated and tested. A three-layer sandwich is fabricated containing micro-resistors, thrust chambers, and rupture diaphragms. A propellant is loaded into each individually sealed chamber. When the resistor is energized, the propellant ignites, raising the pressure in the chamber and rupturing the diaphragm. An impulse is imparted as the high-pressure fluid is expelled from the chamber. On the order of 10^6 thrusters can be fabricated on a single wafer. Initial tests, using lead styphnate as the propellant, have produced 10^{-4} Newton-seconds of impulse and about 100 Watts of power.

Keywords: Micromechanics; Micro-propulsion; Micro-thrusters; Micro-rockets

**Sensors and Actuators A, Physical*, 2000, 80(2), pages 143-154.

†Corresponding author, email: erik@design.caltech.edu

List of Figures

1 Digital micro-Propulsion micro-Spacecraft (Aerospace Corporation [1]). . . 5

2 Digital micro-Propulsion micro-Spacecraft Array (Aerospace Corporation [1]). 6

3 Digital Propulsion micro-Thruster Chip in a 24-pin Ceramic DIP. 7

4 Digital Propulsion micro-Thruster Chip in a 24-pin Ceramic DIP. 8

5 Digital Propulsion micro-Thruster chip, after firing in a vacuum. This image shows the central 3x5 array of thrusters, surrounded by 4 alignment holes. The center-to-center distance between the thrusters is 1 mm. Of the 15 thrusters, 12 fired successfully, and 3 did not fire (apparently, due to corona discharge effects in the firing circuitry). The 3 unfired thrusters are clearly visible: the brightly reflective intact burst diaphragms in the 1st, 3rd and 4th thrusters down in the left-hand column of the 3x5 array. The remnants of the ruptured diaphragms can be seen in the 12 fired thrusters. . . 9

6 Configuration of the Digital Propulsion micro-Thruster Chip. 12

7 Top View of the Digital Propulsion Configuration. 13

8 Top View of a Portion of a Diaphragm Layer Wafer, Containing Six Dies and Showing Three Different Sizes of Burst Diaphragms. 14

9 Top View of a Propellant Layer Wafer Showing Three Different Sizes of Propellant Chambers. The center-to-center distance between the cylindrical chambers is 1 mm. 16

10 Oblique Close-up of Several Dies with Different Sized Propellant Chambers: 700 μm in diameter in the die in the center of the image. The center-to-center distance between the cylindrical chambers is 1 mm. 17

11 Bottom Layer with Resistors. 20

12 CMOS Resistor Design. 21

13 Digital Propulsion micro-Thruster Resistor Energized at 30 volts. This series of images was acquired at 40,500 frames per second. 22

14 Digital Propulsion micro-Thruster Test Stand. 23

15 One frame from a high-speed video of an initial micro-thruster test. In this initial test, the micro-thruster chip was mounted in a chip carrier attached to the stationary aluminum structure on the left side of the image. The thrust from one chamber on the chip propelled the ballistic pendulum (the white structure with the grid) angularly to the right. This image was taken at 1,125 frames per second. 24

16 FIRING THE MICRO-THRUSTER produces, in this early prototype, 0.1 mN of impulse and 100 W of power. The duration of the thrust impulse is about 1 millisecond. The ballistic pendulum (a) is used to precisely measure the thrust produced by the Digital Propulsion chip (b). The thrust plume (c) is visible to the right of the chip. Interferometric optics (d) to measure the displacement of the pendulum are visible in bottom right corner of each frame. This series of images was acquired at 4,500 frames per second. 30

17	Plot of Horizontal Displacement of the Test-Stand Pendulum, from interferometric measurements.	31
18	Plot of an Enlarged Region of the Horizontal Displacement of the Test-Stand Pendulum, from interferometric measurements.	32
19	Plot of Thrust Data for Several micro-Thrusters on a Single Digital Propulsion Chip.	33
20	3-D SIMULATION of a Pair of Cooperating Micro-Spacecraft Controlled by Digital Propulsion micro-Thruster Arrays on each Face. The conical structure extending to from the left-hand micro-spacecraft is a simulated thrust plume. The dots on the faces of the left-hand spacecraft indicate micro-thrusters that have been used. Disturbing forces, including orbital mechanics, require the periodic application of thrust impulses to each spacecraft in order to accurately maintain their positions and orientations.	34

List of Tables

1	Diaphragm	11
2	Plenum	15
3	Resistor	19
4	Propellant	25
5	Repeatability Data for Several micro-Thrusters on a Single Digital Propulsion Chip.	26

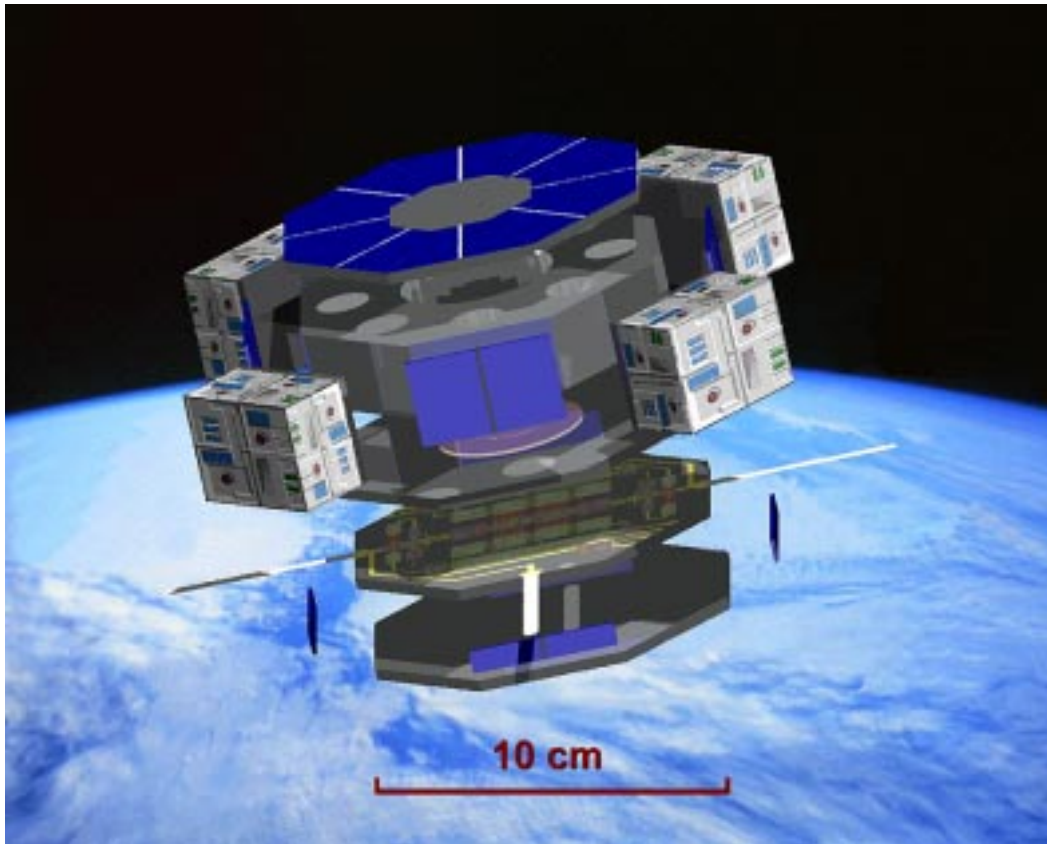


Figure 1: Digital micro-Propulsion micro-Spacecraft (Aerospace Corporation [1]).

1 Introduction

Arrays of one-shot microthrusters fabricated in a three-layer configuration forms the core of the “Digital Propulsion” concept. The three-layer sandwich consists of a top silicon wafer containing burst diaphragms; a middle glass layer containing propellant chambers, and a bottom silicon wafer containing initiators. These micro-thrusters offer new possibilities of increased orbit and station-keeping capabilities, potentially at lower cost. Micro-propulsion is one example of the application of Micro-Electro-Mechanical Systems (MEMS) technology to the space environment, enabling production and deployment of low cost arrays of micro-spacecraft, such as those illustrated in Figures 1 and 2 [1, 2, 3, 4]. This paper describes the Digital Propulsion concept, illustrated in Figures 3 through 5 [5], and reports initial test results.

The objective of this research is to develop thrusters for high-accuracy station-keeping and attitude control of micro-spacecraft. The position and orientation (pointing) accuracy that can be maintained for any spacecraft is determined by its mass (and moments of inertia) and the smallest amount of impulse that can be delivered by its propulsion system. The smallest impulse that can be delivered is referred to as the “impulse bit”. Because the mass

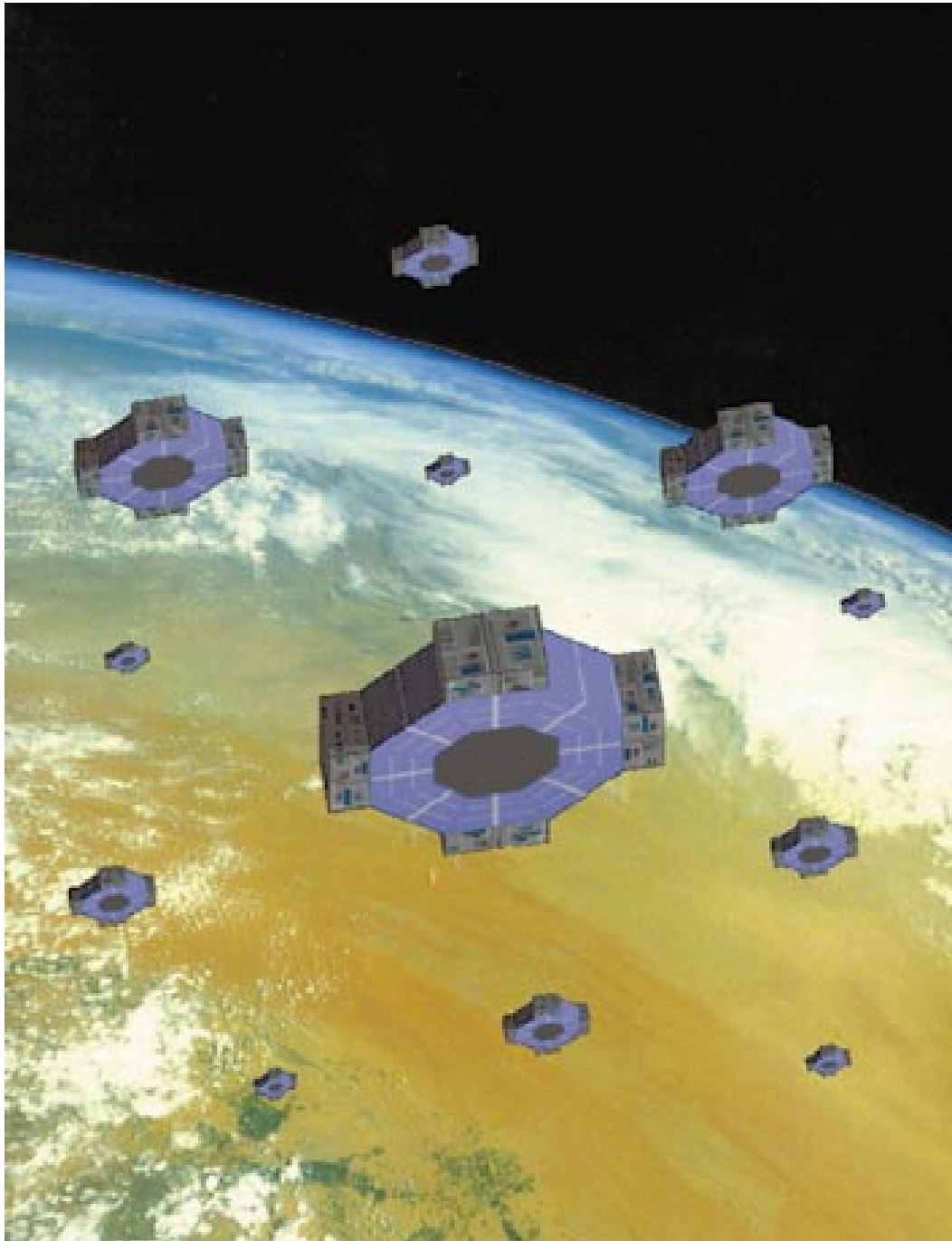


Figure 2: Digital micro-Propulsion micro-Spacecraft Array (Aerospace Corporation [1]).

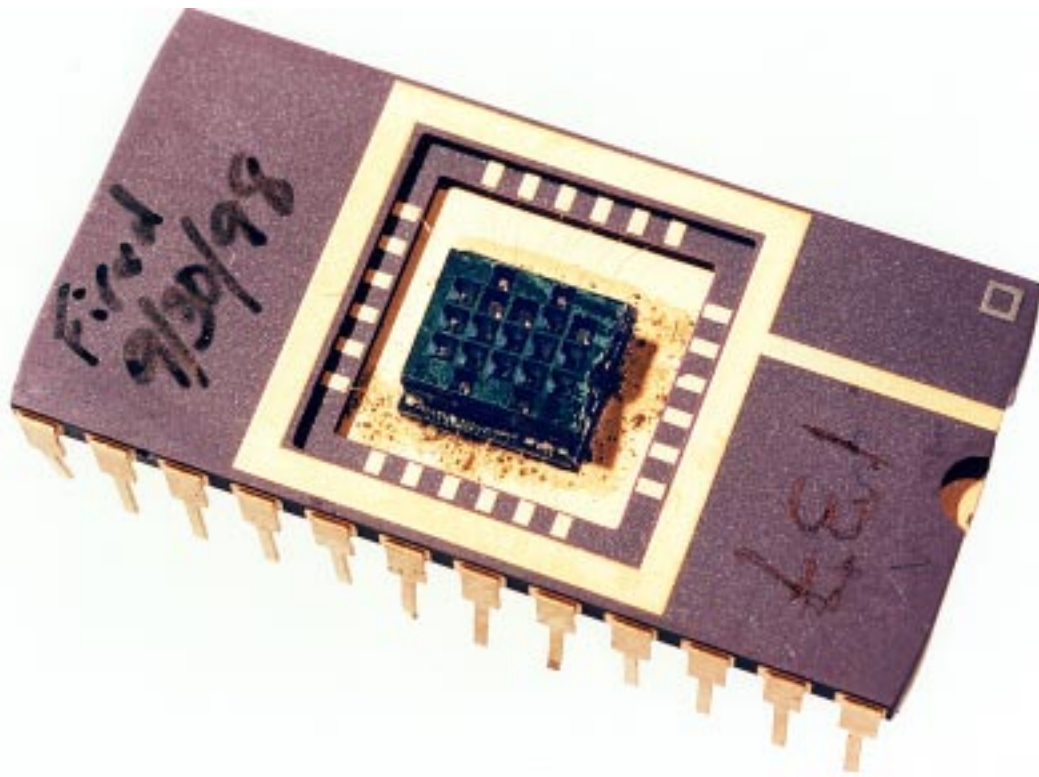


Figure 3: Digital Propulsion micro-Thruster Chip in a 24-pin Ceramic DIP.

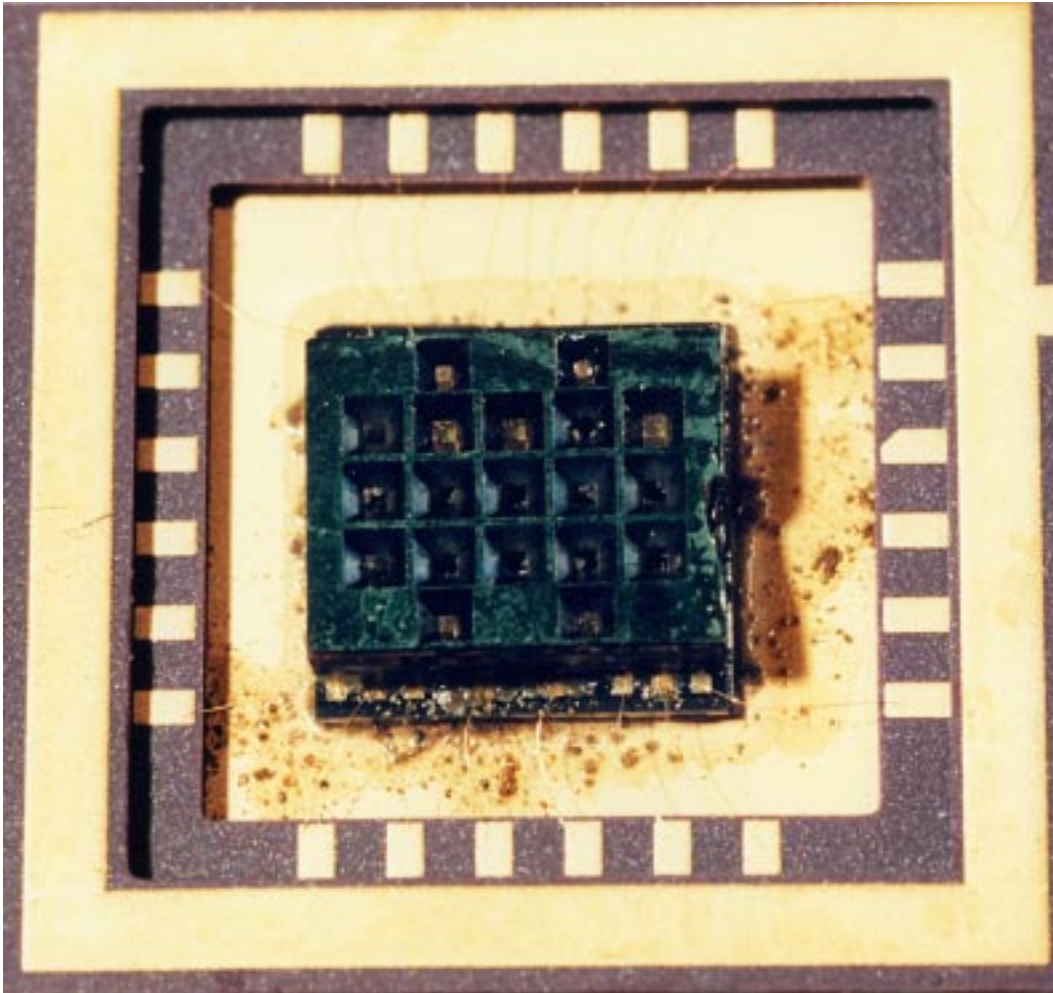


Figure 4: Digital Propulsion micro-Thruster Chip in a 24-pin Ceramic DIP.



Figure 5: Digital Propulsion micro-Thruster chip, after firing in a vacuum. This image shows the central 3x5 array of thrusters, surrounded by 4 alignment holes. The center-to-center distance between the thrusters is 1 mm. Of the 15 thrusters, 12 fired successfully, and 3 did not fire (apparently, due to corona discharge effects in the firing circuitry). The 3 unfired thrusters are clearly visible: the brightly reflective intact burst diaphragms in the 1st, 3rd and 4th thrusters down in the left-hand column of the 3x5 array. The remnants of the ruptured diaphragms can be seen in the 12 fired thrusters.

of a micro-spacecraft is low (*e.g.*, <1 kg), the impulse bit must also be small: on the order of 10^{-4} to $<10^{-6}$ Newton-seconds. Conventional rocket systems, comprising tanks, valves, chambers and nozzles, cannot easily deliver these small impulse bits, and typically require many more components.

2 Configuration

To accomplish these goals, a novel approach to micro-propulsion has been adopted that avoids tanks, fuel lines, and valves. The propulsion system and support structure are fully integrated. In this concept, a sandwich of silicon and glass layers is fabricated to contain an array of small plenums each sealed with a rupturable diaphragm on one side. The plenums are loaded with combustible propellants or an inert substance in gas, liquid or solid form. In the case of a propellant, it is ignited and reacts to form a high-pressure, high-temperature fluid. In the case of an inert substance, it is heated to raise its pressure. Once the pressure exceeds the burst pressure of the diaphragm [6], the diaphragm ruptures, and an impulse is imparted as the fluid is expelled from the plenum. Thus, each plenum can deliver one impulse bit. The size of the impulse is determined during fabrication by the size of the plenum and the propellant that is loaded into it. This approach eliminates valves (and valve leakage). It substitutes one-shot (and therefore consumable) individual thrusters for a multi-use conventional thruster and fuel tank (with a consumable fuel supply). It also integrates spacecraft structure, propellant storage, and thrusters in one multi-layer sandwich.

There are several advantages to this design. These devices have no moving parts, each micro-thruster has a small number of parts ($\simeq 3$), no valves or lines or external tanks. The propulsion function can be combined with the spacecraft structure, by utilizing the structural properties of the multi-layer sandwich. The array of micro-thrusters is highly redundant, individual thrusters can fail, yet the overall capability of the wafer to deliver programmable thrust will be unaffected. The array can be commanded to fire individual thrusters, several thrusters at once, or in controlled sequences, producing controlled, vectored thrust. Since the dimensions of the individual rocket engines are under the designers' control, the creation of smaller and smaller impulse bits is straightforward. On the order of 10^6 thrusters can be fabricated on a single wafer.

The current three-layer sandwich Digital Propulsion configuration is shown in Figure 6. Figure 7 is a top view illustration. The top layer contains an array of thin square diaphragms ($0.5 \mu\text{m}$ thick silicon nitride, 190 or 290 or $390 \mu\text{m}$ on a side, remaining after an anisotropic KOH wet etch through a $\langle 100 \rangle$ silicon wafer). Figure 8 shows a portion of a wafer, from which 3×5 arrays of the three different sized diaphragms are cut. The different sizes were fabricated to evaluate multiple configurations of micro-thrusters.

The middle layer contains an array of through-holes (FOTURAN photosensitive glass, 1.5 mm thick, 300, 500, or $700 \mu\text{m}$ diameter holes) which are loaded with propellant, and is shown in Figures 9 and 10. Three different sizes were fabricated to evaluate different configurations. The dark regions in Figures 9 and 10 have been exposed by a U.V. laser, greatly increasing the rate of HF wet etching in those regions [7].

The bottom layer contains a matching array of polysilicon micro-resistors, and is shown

Table 1: Diaphragm

Material	Silicon Nitride
L	390 μm
Thickness	0.5 μm
Burst Pressure	10 Atm

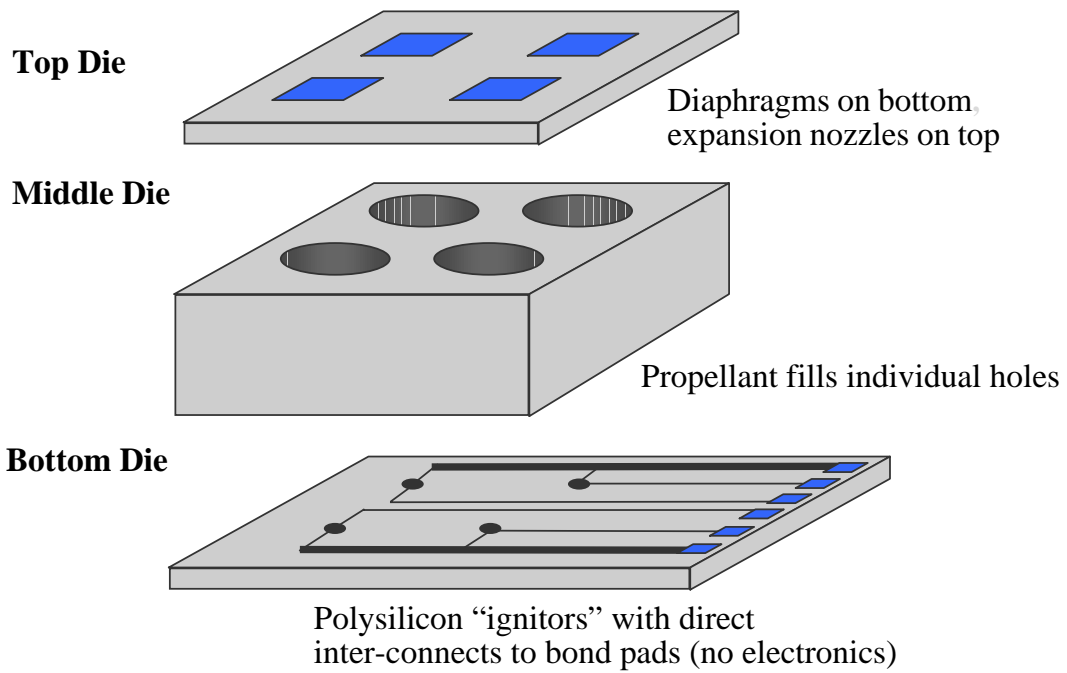


Figure 6: Configuration of the Digital Propulsion micro-Thruster Chip.

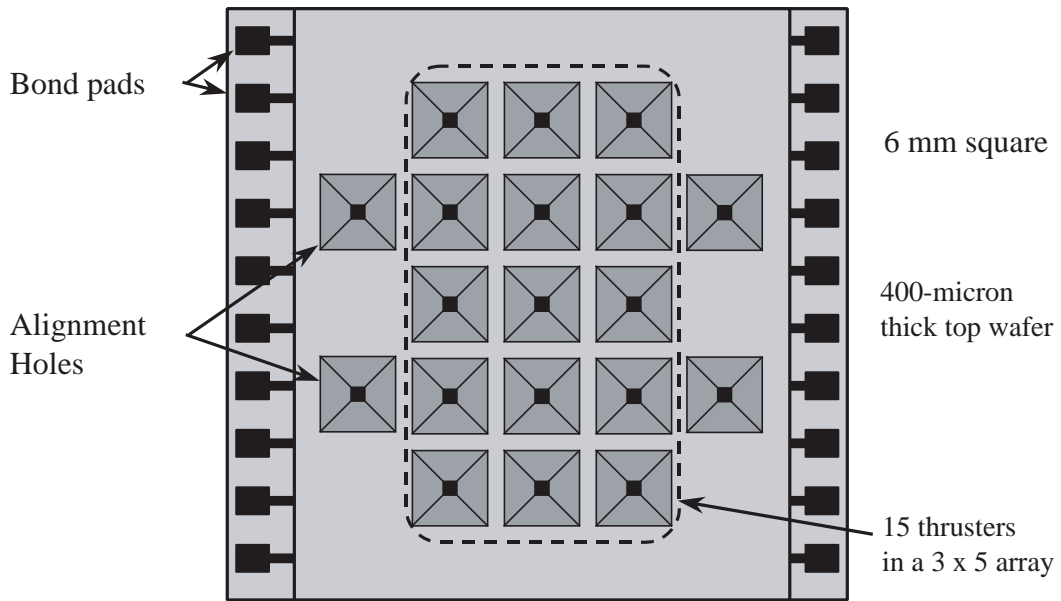


Figure 7: Top View of the Digital Propulsion Configuration.

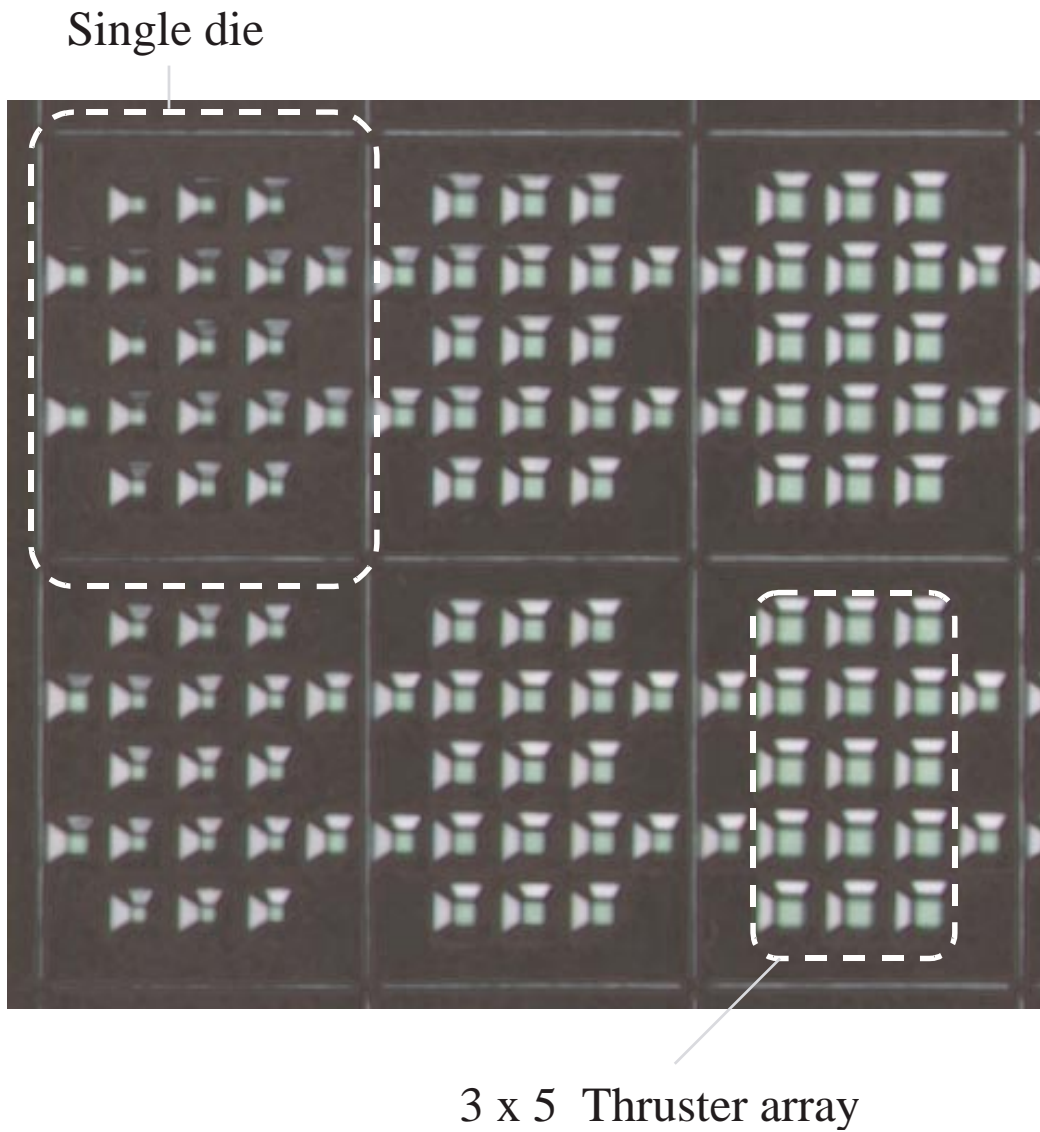


Figure 8: Top View of a Portion of a Diaphragm Layer Wafer, Containing Six Dies and Showing Three Different Sizes of Burst Diaphragms.

Table 2: Plenum

Material	Glass
D	700 μm \emptyset
H	1500 μm

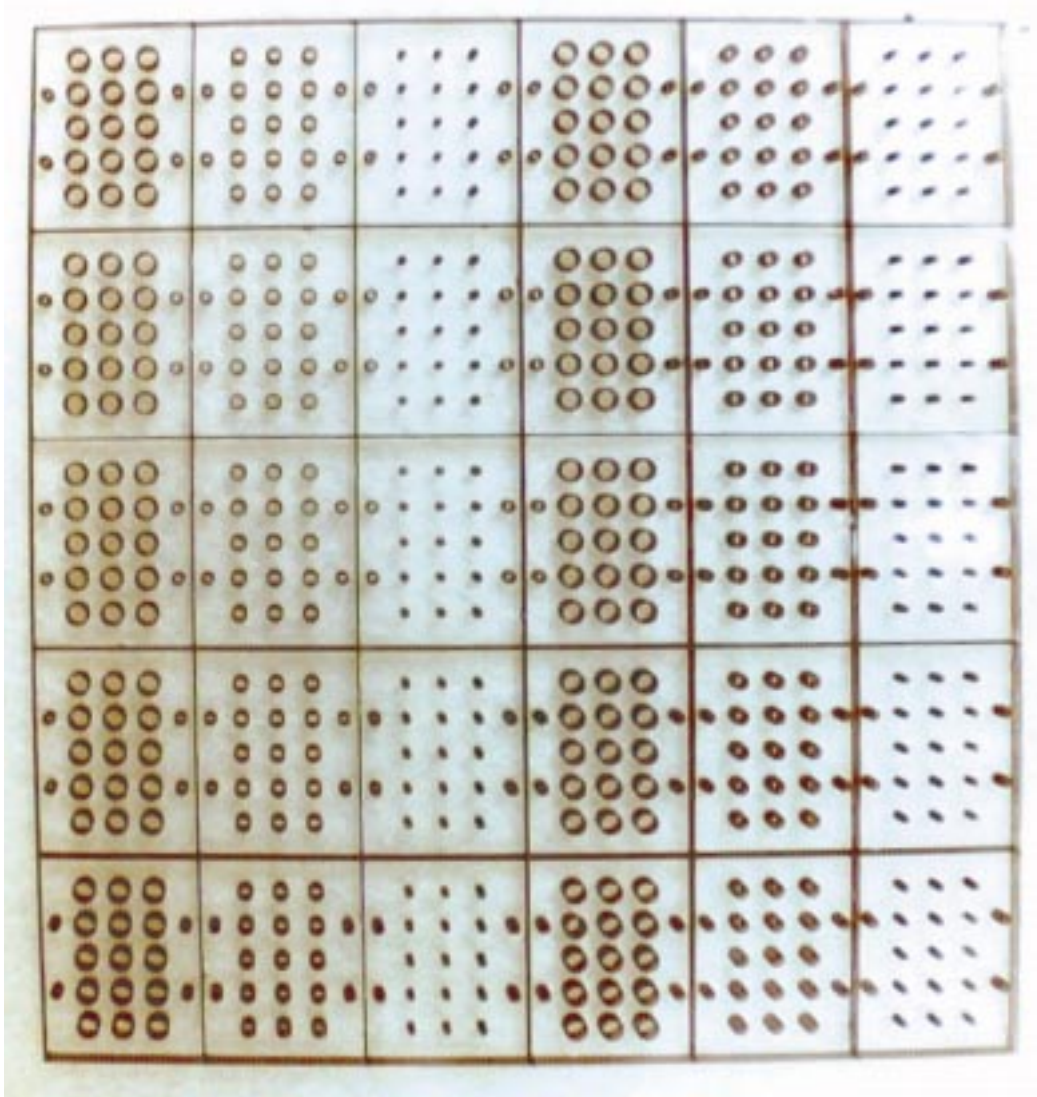


Figure 9: Top View of a Propellant Layer Wafer Showing Three Different Sizes of Propellant Chambers. The center-to-center distance between the cylindrical chambers is 1 mm.

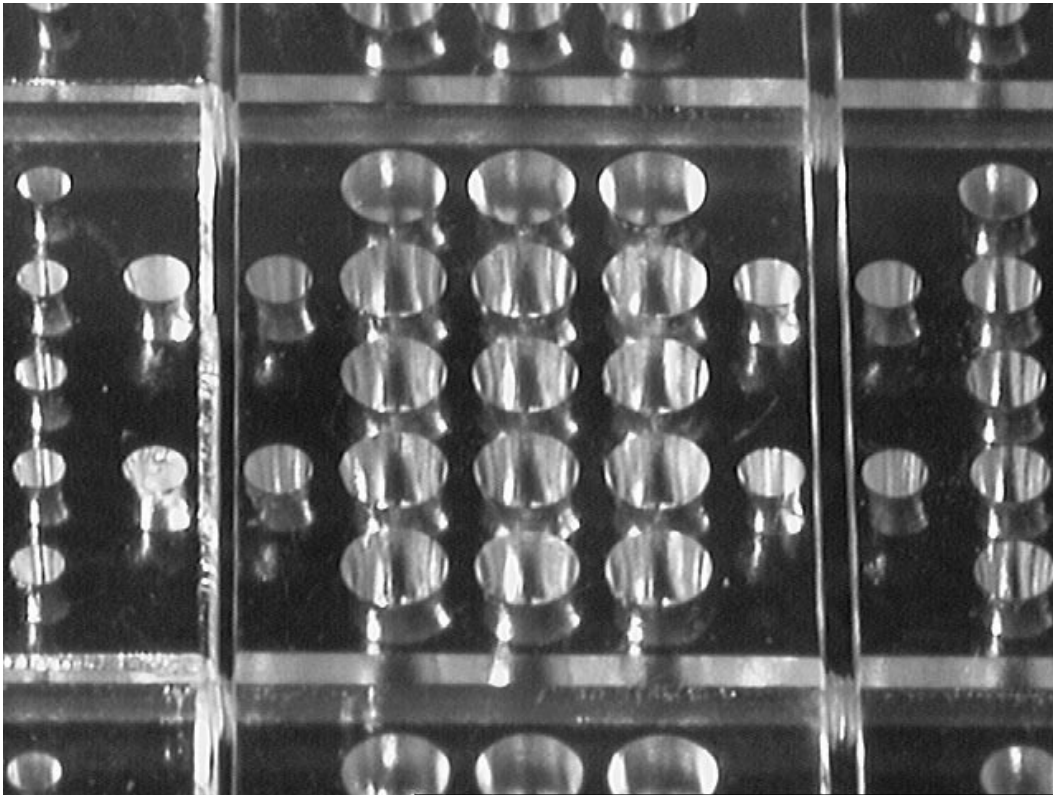


Figure 10: Oblique Close-up of Several Dies with Different Sized Propellant Chambers: 700 μm in diameter in the die in the center of the image. The center-to-center distance between the cylindrical chambers is 1 mm.

in Figure 11. A typical resistor design used here is shown in Figure 12. These resistors are fabricated on top of a 3 μm SiO_2 insulating layer. A series of 8 frames from a high-speed video of a resistor being energized is shown in Figure 13. Since the bottom layer is fabricated using standard CMOS processes, address and control electronics can readily be incorporated into our design. The bottom two layers are bonded together using cyanoacrylate (with alternative bonding methods under consideration), then the chambers are filled with propellant, then the top layer is bonded (also using cyanoacrylate) to complete the assembly. With a series of different sizes of plenum holes, diaphragms, and resistors (as shown in Figures 8 to 11), 90 different configurations of micro-thrusters can be assembled. A completed chip mounted in a 24 pin ceramic dual-inline package (DIP) is shown in Figures 3 through 5.

Table 3: Resistor

Material	Polysilicon
R	210 Ω
V	100 Volts
t	50 μ sec
I	0.5 Amps
Power	50 W
Energy	2.5 mJ

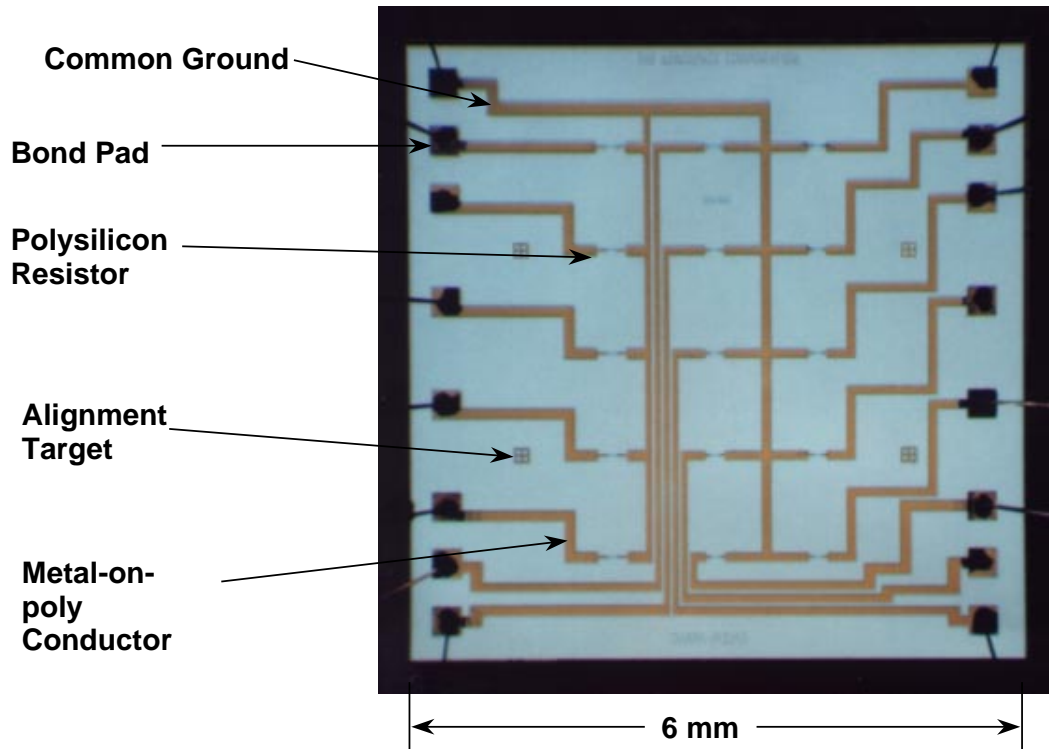


Figure 11: Bottom Layer with Resistors.

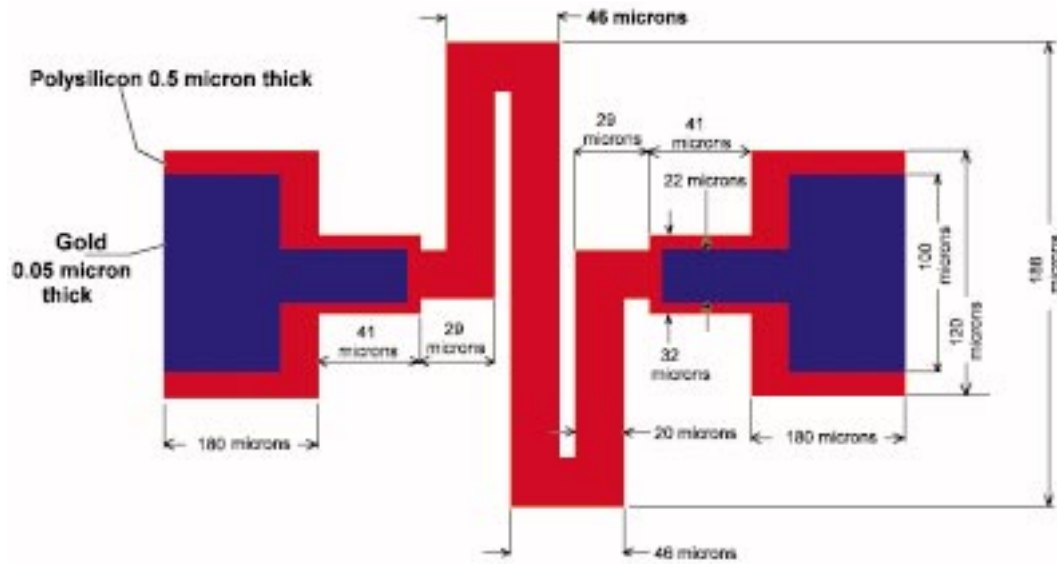


Figure 12: CMOS Resistor Design.

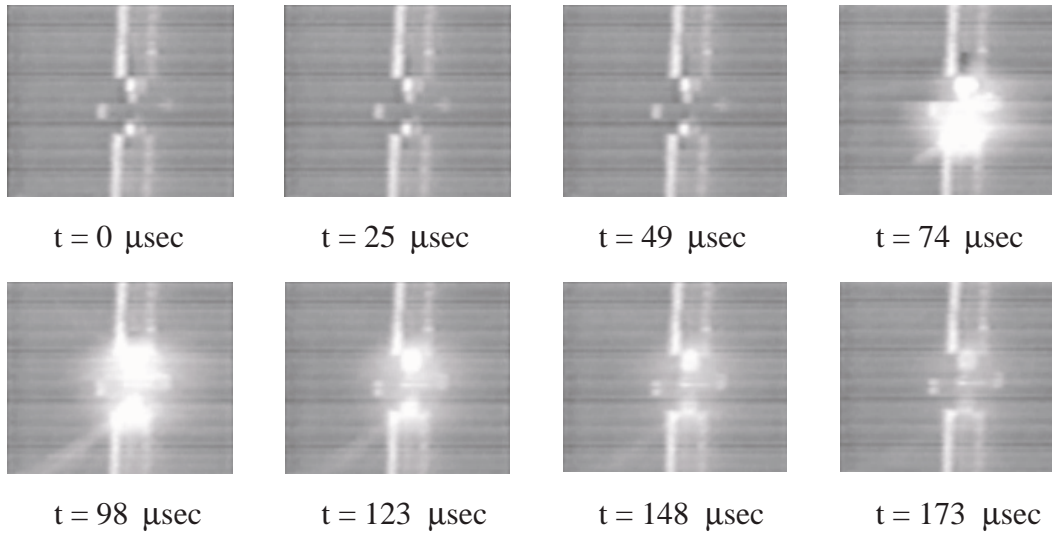


Figure 13: Digital Propulsion micro-Thruster Resistor Energized at 30 volts. This series of images was acquired at 40,500 frames per second.

3 Testing

The test stand for these micro-thruster chips is shown in Figure 14. It includes high-precision low-friction knife-edge pivots; a laser interferometer to accurately measure the displacement history of the ballistic pendulum; an eddy current damper to rapidly restore the pendulum to quiescence after each test; a wireless infra-red data link to communicate with the thrust-initiation electronics; an on-pendulum battery to provide power to the thruster chip; a quick-release 24 pin DIP socket to rapidly change Digital Propulsion chips to be tested, and a vacuum feed-through to permit the thrust tests to be conducted in a vacuum. The test stand is calibrated with a track and a series of solenoids to release metal calibration spheres from known positions.

One frame from a high-speed video of an initial micro-thruster test is shown in Figure 15. A series of 7 frames from a high-speed video of a later micro-thruster test is shown in Figure 16. This latest series of tests, using lead styphnate as the propellant, has produced 10^{-4} Newton-seconds of impulse and about 100 Watts of power. As can be seen in Figure 16, the duration of the thrust impulse from each chamber is about 1 millisecond. A ballistic pendulum is used to precisely measure the thrust produced. The thrust plume (labeled (c) in the diagram at the top of Figure 16) is visible to the right of the chip. At $t = -0.22$ msec the firing sequence has not yet begun. At $t = 0.00$ msec the resistor is energized and the combustion of the propellant begins, rupturing the burst diaphragm and producing the visible thrust plume. At each successive time, the plume appears smaller and less bright, indicating the progress of the combustion process. Finally, by $t = +1.11$ msec the combustion is complete, and the impulse of thrust has been delivered. The pendulum, to which the Digital Propulsion chip is mounted, has sufficient mass that it has not yet moved

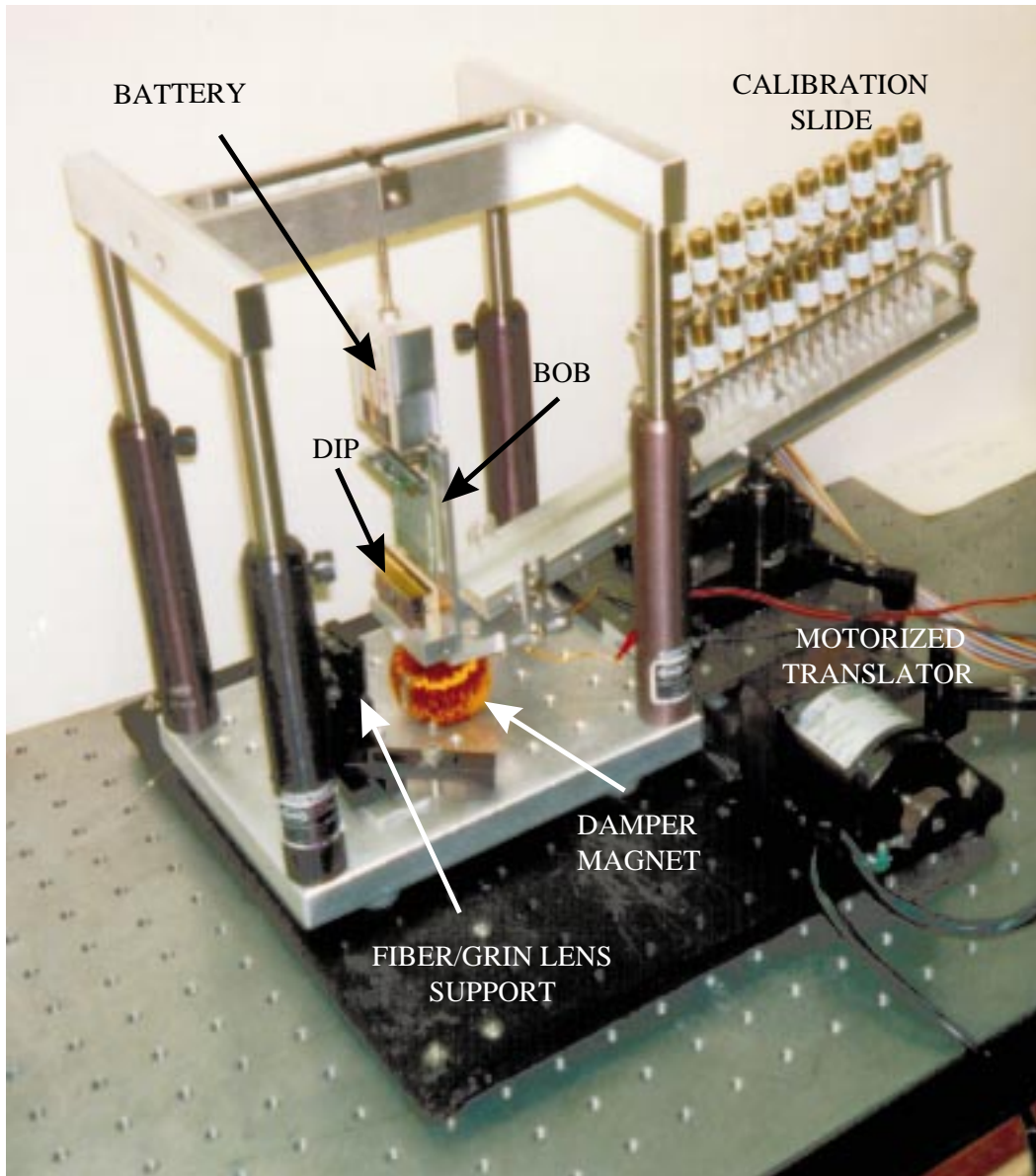


Figure 14: Digital Propulsion micro-Thruster Test Stand.

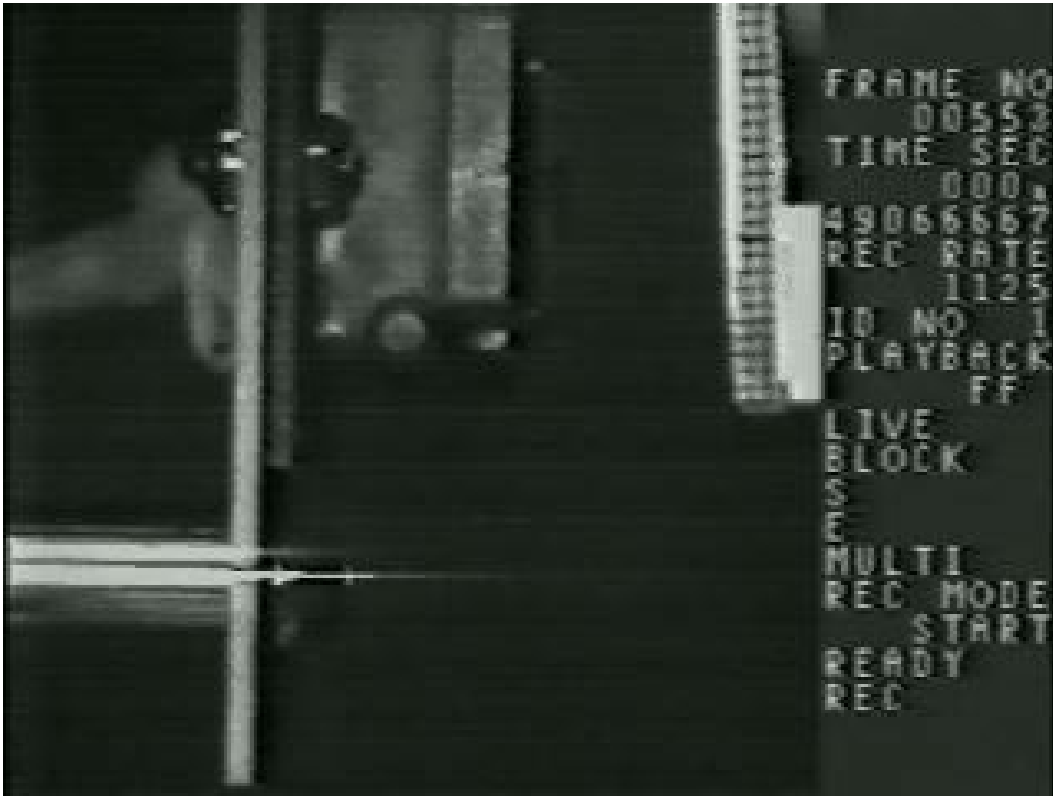


Figure 15: One frame from a high-speed video of an initial micro-thruster test. In this initial test, the micro-thruster chip was mounted in a chip carrier attached to the stationary aluminum structure on the left side of the image. The thrust from one chamber on the chip propelled the ballistic pendulum (the white structure with the grid) angularly to the right. This image was taken at 1,125 frames per second.

an amount visible in the video image. Typical pendulum displacements reach $130 \mu\text{m}$. Thermochemistry calculations, confirmed in-part by the brightness of the thrust plume, have shown that only about 10% of the propellant has produced thrust [8]. Our expectation is that this can be increased by nearly a factor of 10 with more complete combustion of the propellant. Figure 17 shows the horizontal displacement of the test-stand pendulum as a result of the firing of micro-thruster #11 on Digital Propulsion chip #3. Figure 18 shows an enlarged region of the horizontal displacement for an earlier test, showing the excitation of the pendulum dynamics. Table 5 and Figure 19 show the repeatability of thrust produced on a single chip.

Additional tests using inert gases, vaporizing liquids and several types of solid propellants have been conducted.

Table 4: Propellant

Material	Lead Styphnate
Class	1.3
F	0.1 T
t	1 msec
Impulse	0.1 mN-sec
Power	100 W
Energy	100 mJ

Table 5: Repeatability Data for Several micro-Thrusters on a Single Digital Propulsion Chip.

Thruster #	Impulse %Avg	Error %Avg
7	114.21	001.13
8	099.02	002.81
9	088.51	005.06
10	095.08	002.81
11	099.14	003.94
12	092.83	002.81
13	119.83	003.38
14	102.39	002.81

4 Simulation

A series of simulations of micro-spacecraft have been performed to evaluate the efficacy of small one-shot impulses from arrays of micro-thrusters for station-keeping and attitude control. A simple “opportunistic” controller was implemented that at each time step evaluates how well each remaining thruster can correct the position, orientation and velocity error of the spacecraft. The simulation models both the nominal impulse, plus adds a random variation in both direction and magnitude. Disturbing forces are also applied to each micro-spacecraft, modeling both quasi-constant forces (such as solar pressure and atmospheric drag) and random impulses (such as nano-meteorites). Because orbital mechanics will impose relative motion of two spacecraft [9], these effects have also been incorporated into the simulation.

Initial simulation results suggest that the Digital Propulsion micro-thruster approach can provide sub-millimeter station-keeping for 1 kg micro-spacecraft at orbits above 100 km. One frame from a simulation is shown in Figure 20.

5 Conclusions

The design and configuration of initial prototypes of Digital Propulsion micro-thruster chips are described. The three-layer sandwich consists of a top silicon wafer containing burst diaphragms; a middle glass layer containing propellant chambers, and a bottom silicon wafer containing initiators. Initial thrust test data is reported, including time-histories of test-stand pendulum displacement. Using a solid propellant, initial tests have developed 10^{-4} Newton-seconds of impulse and about 100 Watts of power.

Acknowledgements

This material is based upon work supported, in part, by the Defense Advanced Research Projects Agency (DARPA), Microsystems Technology Office (MTO), MEMS Program, directed by Dr. Al Pisano under Contract N66001-97-C-8609 administered by SPAWAR Systems Center San Diego, Electromagnetics and Advanced Technology Division, Code D8505. Any opinions, findings, conclusions, or recommendations expressed in this publication are those of the authors and do not necessarily reflect the views of the sponsor(s).

We acknowledge the efforts of Henry Helvajian, William Hansen, Edward J. Beiting III, Brian B. Brady, Peter Fuqua and Meg Abraham at the Aerospace Corporation in fabricating and testing the thrusters, and Charles Kim, Mark Long and Lin Ma at the California Institute of Technology in developing the simulations and performing analyses of the thrusters.

Biographies

David H. Lewis, Jr. received his Ph.D. degree from MIT and has over 20 years experience in research and development of innovative technology related to rocket propulsion systems and gas dynamics. He is the manager of the DARPA-sponsored MEMS Digital Propulsion project. He is the co-author on liquid propulsion in the recently published book *Space Propulsion Analysis and Design*. In addition, he has taught numerous university level courses in rocket propulsion, heat transfer, thermodynamics, system dynamics, and fuzzy logic systems at Caltech and UCLA. Dr. Lewis is a past winner of the TRW Chairman's Award for Innovation.

Siegfried W. Janson Dr. Siegfried Janson is a senior scientist at the Aerospace Corporation. He obtained a Bachelor of Science degree in aeronautical engineering in 1977 from Rensselaer Polytechnic Institute, a Master of Engineering degree in aerospace engineering in 1978 from Cornell University, and a Ph.D. in aerospace engineering from Cornell University in 1984. He was a post-doctoral associate at Cornell from 1984 to 1987, at which time he joined the Aerospace Corporation to pursue experimental research in electric thrusters for spacecraft. Dr. Janson's current research interests are micropropulsion, microelectromechanical systems for spacecraft, and silicon satellites ("nanosats"). He invented the silicon nanosatellite in 1989 and has published over 15 papers on their propulsion requirements, basic design issues, and orbital architecture. He is a member of the IEEE and a senior member of the American Institute of Aeronautics and Astronautics (AIAA).

Erik K. Antonsson received the B.S. degree from Cornell University (1976), and the S.M. (1978) and Ph.D. (1982) degrees from M.I.T., Cambridge, MA, all in Mechanical Engineering. In September 1984 he joined the faculty of the California Institute of Technology, where he is currently Executive Officer and Professor of Mechanical Engineering. He teaches courses in engineering design, computer aided engineering design, mechanical systems, and kinematics. His research interests include formal methods for engineering design, representing and manipulating imprecision in preliminary engineering design, and structured design of micro-electro-mechanical systems (MEMS). He was an NSF Presidential Young Investigator from 1986 to 1992, and was awarded the Richard P. Feynman Prize for Excellence in Teaching in 1995. Dr. Antonsson is a member of the ASME, IEEE, SME, ASEE, IFES, and NAFIPS. He is currently on the editorial board of the International Journals: *Fuzzy Sets and Systems*, and *Research in Engineering Design*, and served as a Associate Technical Editor for the ASME *Journal of Mechanical Design*, (formerly the *Journal of Mechanisms, Transmissions and Automation in Design*), with responsibility for the Design Research and the Design Theory and Methodology area, from 1989 to 1993.

References

- [1] S. W. Janson. Chemical and electric micropropulsion concepts for nanosatellites. In *Proceedings of the 30th AIAA/ASME/SAE/ASEE Joint Propulsion Conference*, Indianapolis, IN, June 1994. Paper AIAA-94-2998.
- [2] S. W. Janson, H. Helvajian, and E. Y. Robinson. The concept of 'nanosatellite' for revolutionary low-cost space systems. In *Proceedings of the 44th International Astronautics Federation Conference*, Graz, Austria, Oct. 1993. Paper IAF-93-U.5.573.
- [3] S. W. Janson and H. Helvajian. Batch-fabricated microthrusters: Initial results. In *Proceedings of the 32nd AIAA/ASME/SAE/ASEE Joint Propulsion Conference*, Lake Buena Vista, FL, June 1996. Paper AIAA-96-2988.
- [4] S. W. Janson and H. Helvajian. Batch-fabricated microthrusters for kilogram-class spacecraft. In *Proceedings of Government Microcircuit Applications Conference*, Arlington, VA, Mar. 1998.
- [5] D. H. Lewis, Jr., S. W. Janson, R. B. Cohen, and E. K. Antonsson. Digital MicroPropulsion. In *The Twelfth IEEE International Micro Electro Mechanical Systems Conference*, Orlando, Florida, Jan. 1999. IEEE.
- [6] S. Timoshenko. *Theory of Plates and Shells*. McGraw-Hill, New York, 1940.
- [7] W. W. Hansen and S. W. Janson. Direct-write UV laser microfabrication of 3D structures in lithium-alumosilicate glass. In *SPIE Proceedings Volume 2991*, page 104, 1997.
- [8] A. H. Shapiro. *The Dynamics and Thermodynamics of Compressible Fluid Flow*. Ronald Press Co., New York, 1953-54.
- [9] V. A. Chobotov, editor. *Orbital Mechanics*. AIAA American Institute of Aeronautics and Astronautics, Inc., Reston, VA, 1996.

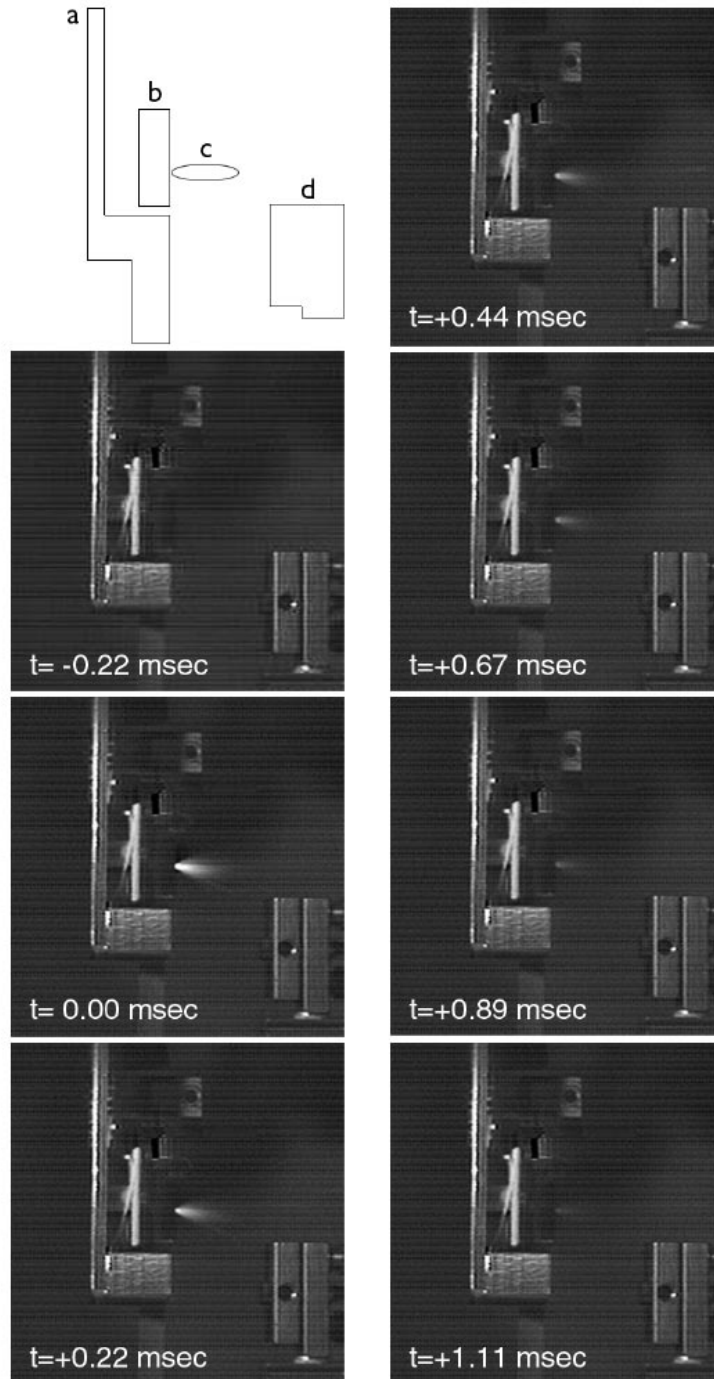


Figure 16: FIRING THE MICRO-THRUSTER produces, in this early prototype, 0.1 mN of impulse and 100 W of power. The duration of the thrust impulse is about 1 millisecond. The ballistic pendulum (a) is used to precisely measure the thrust produced by the Digital Propulsion chip (b). The thrust plume (c) is visible to the right of the chip. Interferometric optics (d) to measure the displacement of the pendulum are visible in bottom right corner of each frame. This series of images was acquired at 4,500 frames per second.

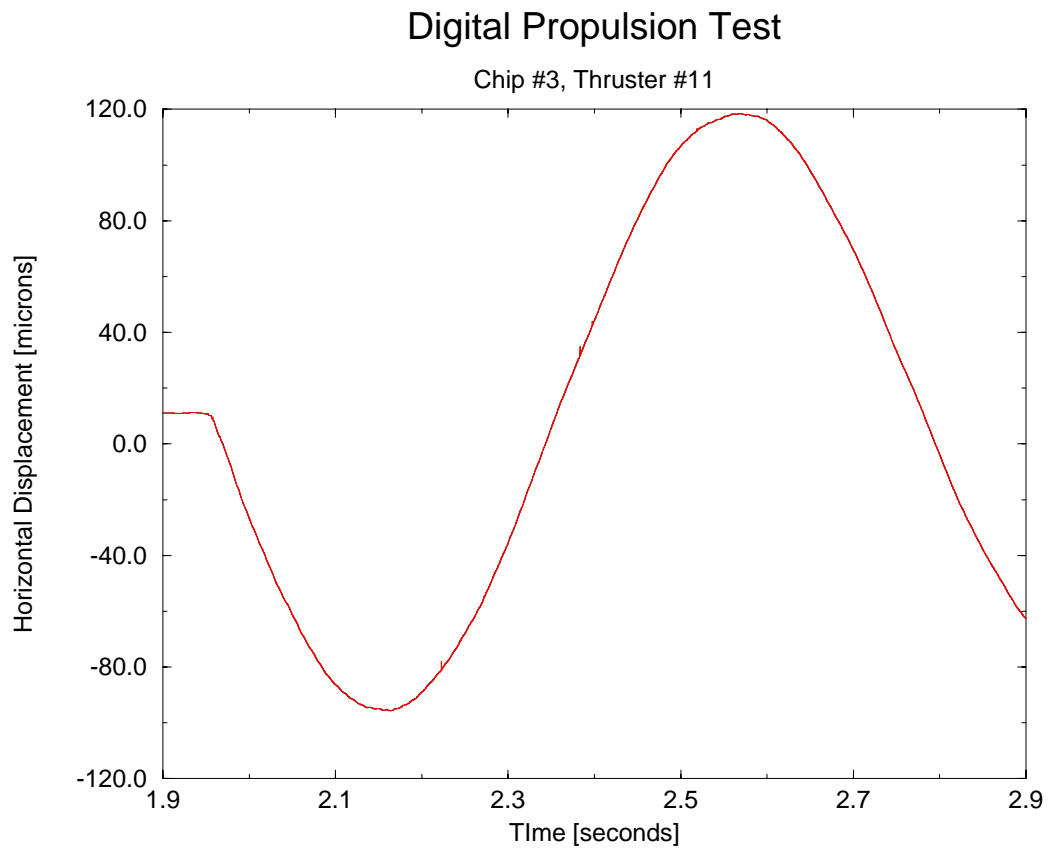


Figure 17: Plot of Horizontal Displacement of the Test-Stand Pendulum, from interferometric measurements.

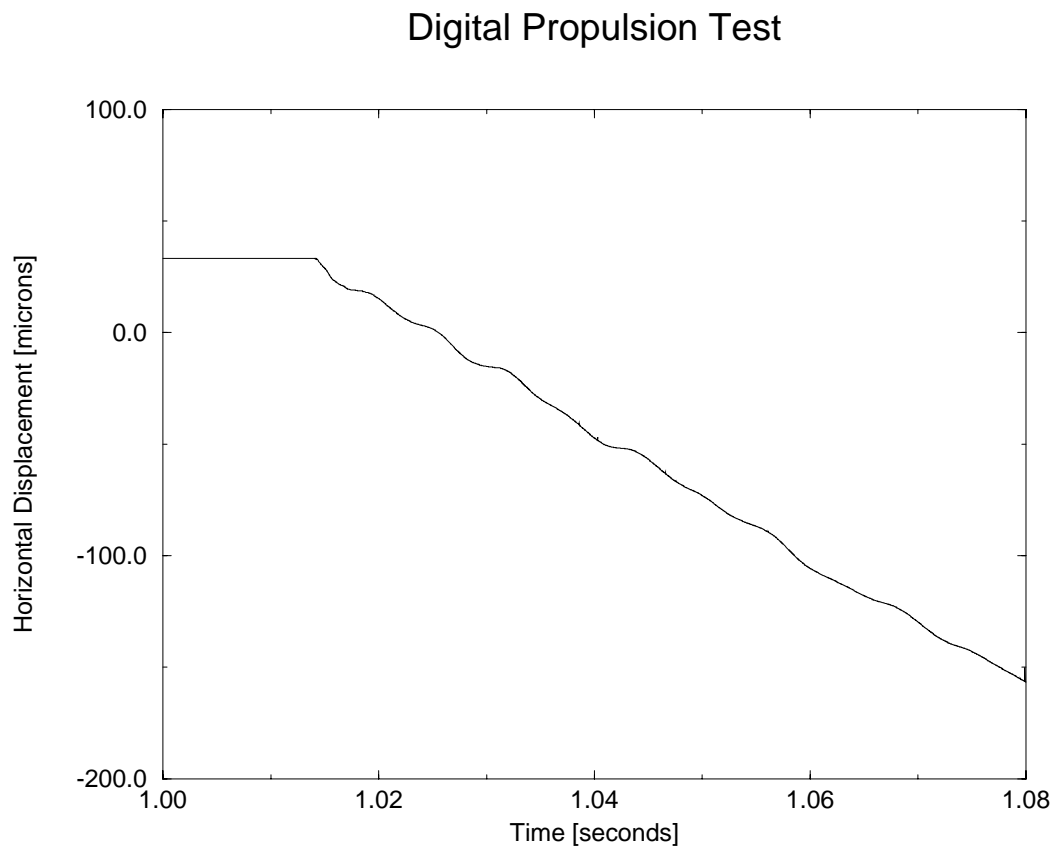


Figure 18: Plot of an Enlarged Region of the Horizontal Displacement of the Test-Stand Pendulum, from interferometric measurements.

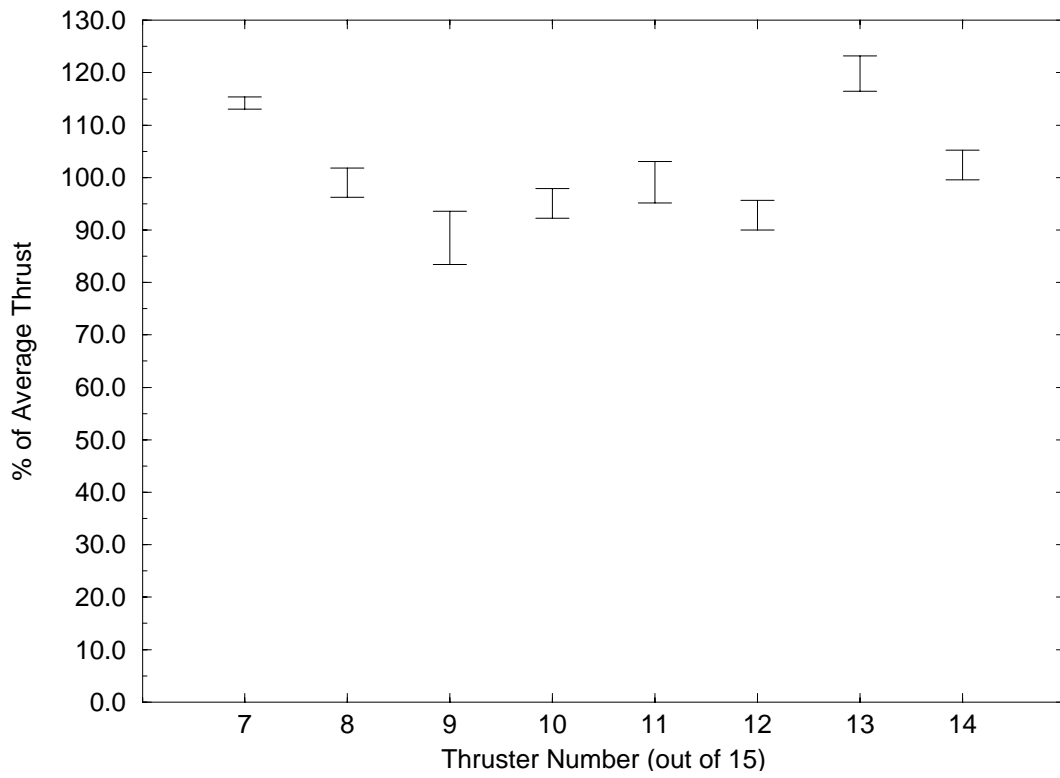


Figure 19: Plot of Thrust Data for Several micro-Thrusters on a Single Digital Propulsion Chip.

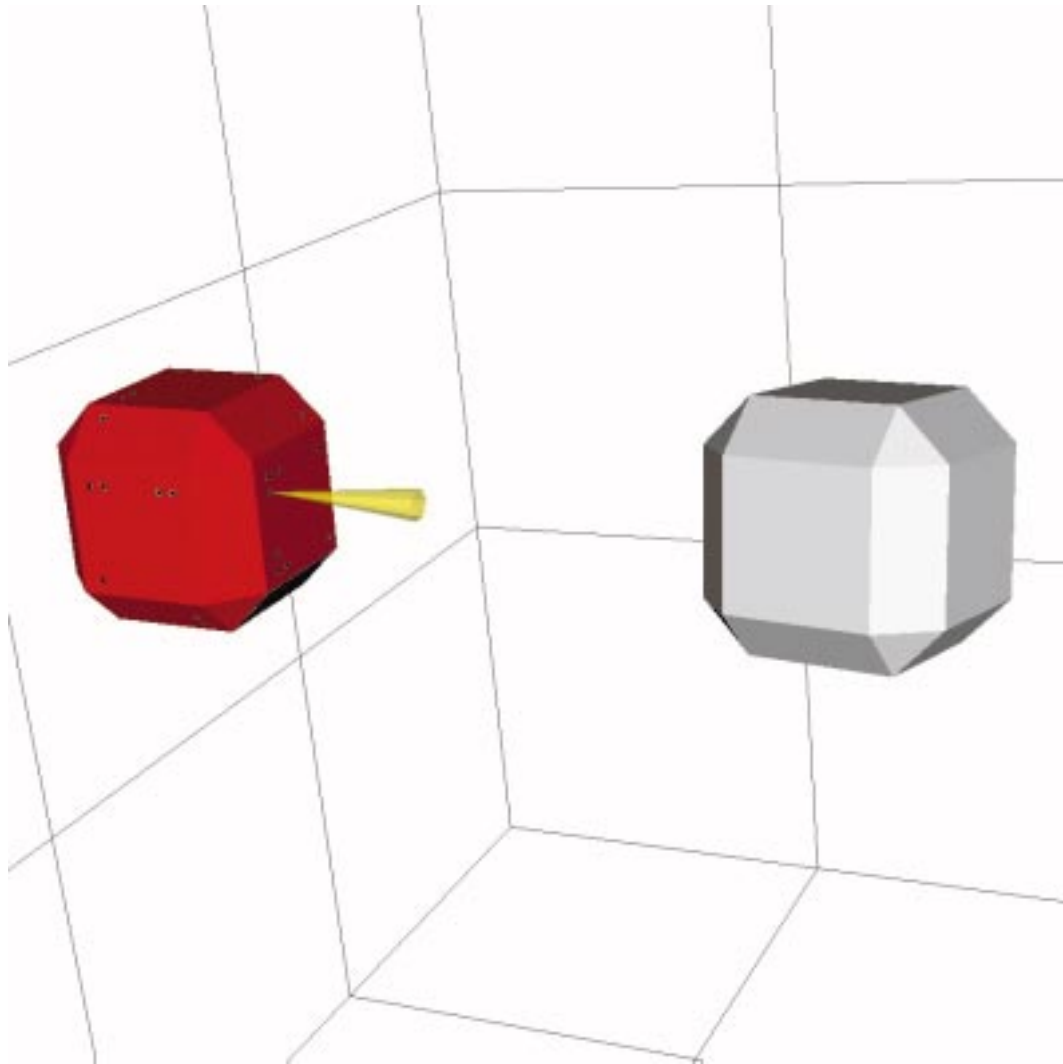


Figure 20: 3-D SIMULATION of a Pair of Cooperating Micro-Spacecraft Controlled by Digital Propulsion micro-Thruster Arrays on each Face. The conical structure extending to from the left-hand micro-spacecraft is a simulated thrust plume. The dots on the faces of the left-hand spacecraft indicate micro-thrusters that have been used. Disturbing forces, including orbital mechanics, require the periodic application of thrust impulses to each spacecraft in order to accurately maintain their positions and orientations.